Supporting Information

Bouldin et al. 10.1073/pnas.0912818107

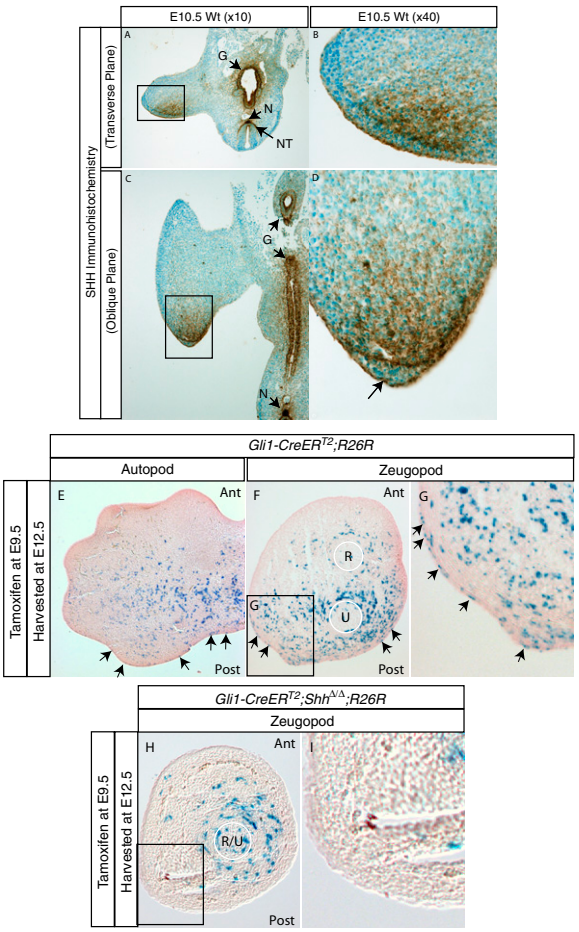

Fig. S1. SHH immunohistochemistry on E10.5 embryos. To confirm the ectodermal immunoreactivity of SHH and the specificity of the antibody, limb buds were analyzed using different planes of section. (*A*) Embryos at E10.5 cut at the transverse plane of section showed immunoreactivity of SHH in several tissues known to be positive for SHH including the gut (G), the notochord (N), the neural tube (NT), and the posterior region of the limb including the ectoderm. The box in *A* is enlarged in *B*. (*C*) Similarly, embryos at E10.5 cut on an oblique plane of section showed the immunoreactivity of SHH in tissues known to express *Shh* and in the posterior region of the limb including the ectoderm. The box in *C* is enlarged in *D*. The arrow in *D* highlights SHH immunostaining in the AER. (*E*–*I*) Fate-mapping of cells responding to Hh signal transduction in limbs exposed to Tamoxifen at E9.5 and harvested at E12.5. Sectioned limbs of *Gli1-CreER^{T2};R26R* embryos showed descendants of cells responding to Hh signal transduction in the posterior mesoderm and posterior ectoderm of the autopod (*E*) and zeugopod (*F* and *G*) (1). To determine whether the ectodermal staining observed in *Gli1-CreER^{T2};R26R* embryos required SHH, fate mapping of *Gli1*-expressing cells was repeated in *Shh* null (*Shh$^{\Delta/\Delta}$*) embryos. (*H* and *I*) Sectioned *Shh$^{\Delta/\Delta}$* limbs containing the *Gli1-CreER^{T2}* and *R26R* alleles showed no cells that had responded to Hh signal in the ectoderm of the zeugopod. Cells surrounding the cartilaginous elements in the limb mesoderm expressed *Gli1* in the absence of SHH indicating activation of the Hh signaling pathway in this region of the limb. This staining is likely the result of IHH activation of the Hh signaling pathway because *Ihh* is expressed in chondrocytes (2, 3). These data indicate that ectodermal cells have activated the Hh signaling pathway in response to SHH produced from the ZPA.

1. Ahn S, Joyner AL (2004) Dynamic changes in the response of cells to positive hedgehog signaling during mouse limb patterning. *Cell* 118:505–516.
2. Bitgood MJ, McMahon AP (1995) Hedgehog and Bmp genes are coexpressed at many diverse sites of cell-cell interaction in the mouse embryo. *Dev Biol* 172:126–138.
3. St-Jacques B, Hammerschmidt M, McMahon AP (1999) Indian hedgehog signaling regulates proliferation and differentiation of chondrocytes and is essential for bone formation. *Genes Dev* 13:2072–2086.

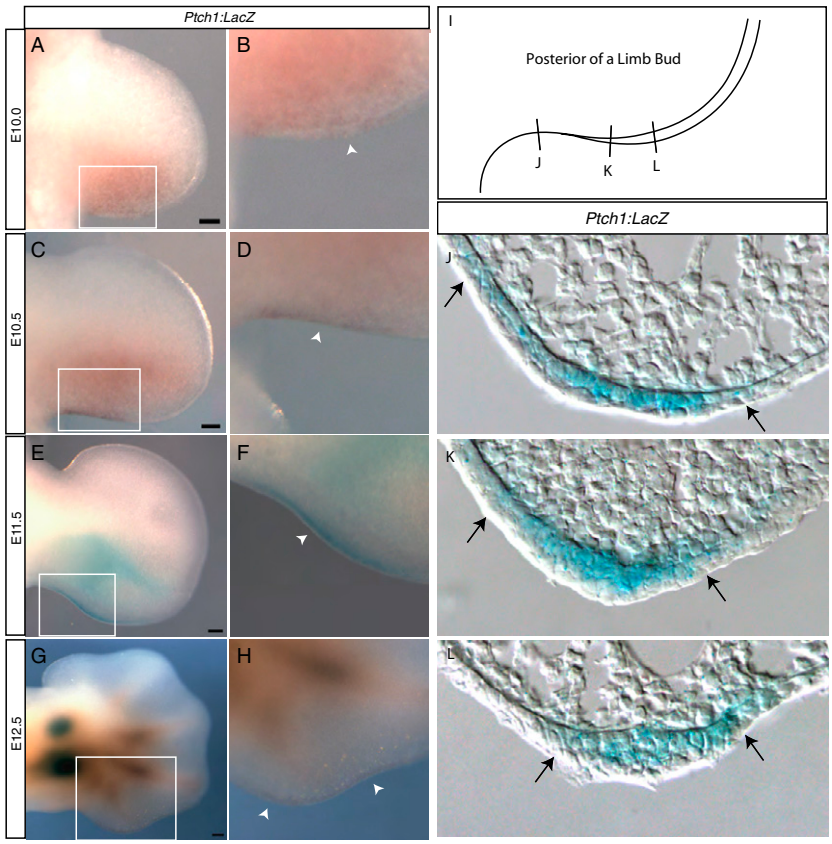

Fig. S2. *Ptch1:LacZ* expression in limb buds. To expand our analysis of *Ptch1* expression in the limb bud ectoderm, we analyzed *Ptch1:LacZ* embryos at various stages. (*A*) At E10.0, β-galactosidase activity was punctate in the posterior of the developing limb. (*B*) At a higher magnification, β-galactosidase activity was present in the posterior of the developing limb including the ectoderm (highlighted by an arrowhead). (*C* and *E*) At E10.5 and E11.5, β-galactosidase activity was present in the posterior of the limb. Higher magnification revealed robust staining in the ectoderm (*D* and *F*; highlighted by an arrowhead). (*G*) At E12.5, β-galactosidase activity was no longer posteriorly restricted in the mesoderm and was found surrounding proliferating chondrocytes, a known source of *Ihh*. (*H*) At high magnification in the E12.5 limb, β-galactosidase activity persisted in the posterior ectoderm (highlighted by arrowheads). Additional sagittal sections from embryos containing the *Ptch1:LacZ* allele at E11.5 were also analyzed. (*I*) A schematic of the posterior of the developing limb bud showing approximate locations of sectioned tissue. (*J*) In a section from the posterior margin (the posterior region from the flank to the AER), β-galactosidase activity was detectable in the posterior ectoderm including portions of the dorsal and ventral ectoderm. (*K*) In a section from the proximal portion of the posterior AER, β-galactosidase activity was detectable in the ectoderm including the AER. (*L*) A section from a more distal portion of the posterior AER revealed β-galactosidase activity exclusively in the AER. Arrows mark the dorsal and ventral extremes of detectable β-galactosidase activity in the ectoderm.

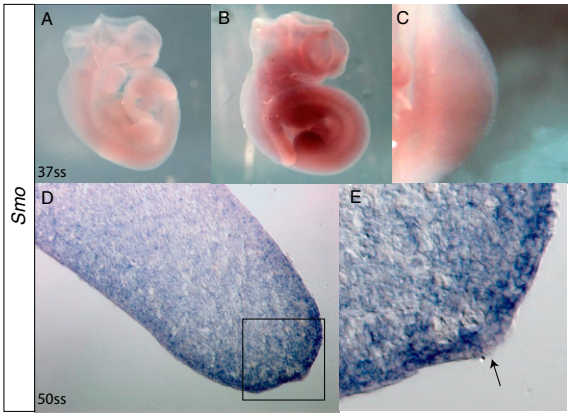

Fig. S3. *Smo* expression in the embryo including the AER of the developing limb at E10.5. To investigate the presence of *Smo* in the embryo, a series of RNA in situ hybridizations were performed by using a riboprobe designed to detect *Smo*. At 37ss, embryos hybridized to a sense probe revealed no staining (*A*); however, embryos stained with an antisense probe designed to recognize *Smo* mRNA identified expression in a large number of tissues throughout the embryo (*B*), including the limb (*C*). Tissue harvested at 50ss and sectioned revealed staining throughout the mesoderm and ectoderm of the limb including the AER (*D*). The boxes in *D* are enlarged in *E*. The arrow in *E* highlights *Smo* expression in the AER.

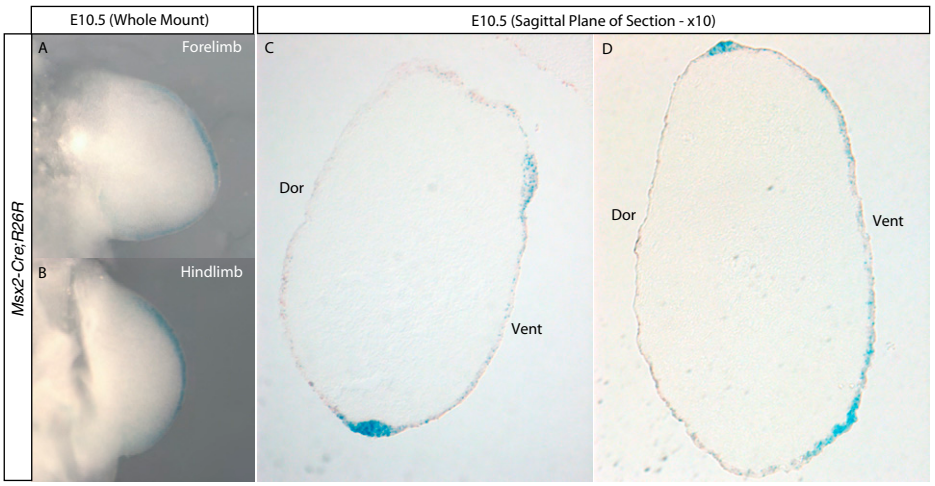

Fig. S4. *Msx2-Cre* is expressed robustly in the AER and not in the limb bud mesoderm. To investigate the expression of *Msx2-Cre* in the developing limb, mating schemes were designed to incorporate the *Rosa26* reporter into animals with the *Msx2-Cre* allele. In these limbs, cells that have β-galactosidase activity have at some time during development expressed cre recombinase from the *Msx2-Cre* allele. At E10.5, *Msx2-Cre* was expressed in the AER of both forelimbs (*A*) and hindlimbs (*B*). Sagittal sections of E10.5 limbs revealed β-galactosidase activity in the AER and ventral ectoderm of two different limbs (*C* and *D*). In all of the limbs analyzed, β-galactosidase activity was restricted to the ectoderm.

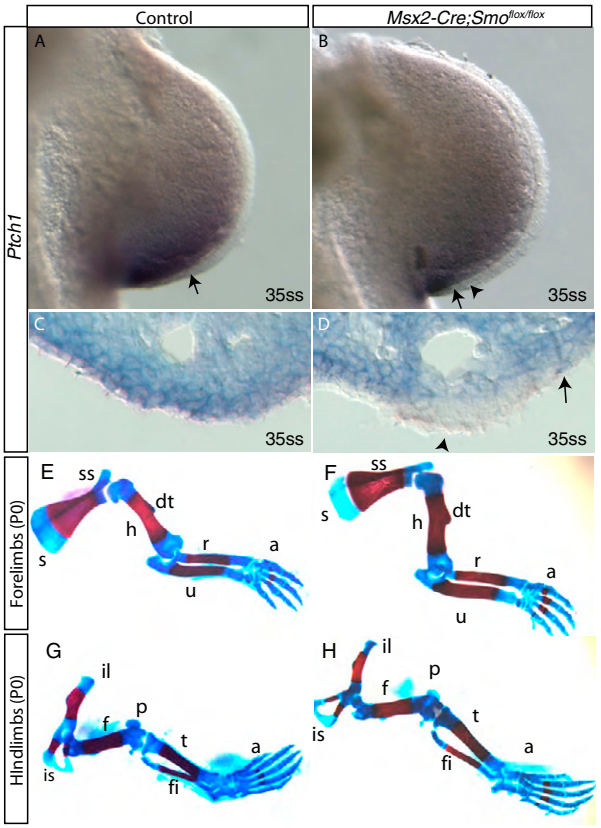

Fig. S5. *Ptch1* is lost from the AER at E10.5 of *Msx2-Cre;Smo*$^{flox/flox}$ limb buds. To expand our analysis of the loss of Shh signaling in the developing limb ectoderm, we analyzed expression of *Ptch1* by whole-mount RNA in situ hybridization. (*A*) *Ptch1* was expressed throughout the posterior of the control limb at 35ss including the ectoderm. (*B*) In *Msx2-Cre;Smo*$^{flox/flox}$ limbs at 35ss, *Ptch1* was expressed in the posterior limb bud mesoderm and in the most proximal region of the posterior ectoderm, but was not expressed in the AER. Sectioned limbs revealed that *Ptch1* was present in posterior ectoderm of control limbs (*C*), but absent from the AER of *Msx2-Cre;Smo*$^{flox/flox}$ limbs (*D*). The arrowhead denotes loss of expression in the AER, whereas the arrow marks expression in ectoderm adjacent to the AER. (*E–H*) Skeletal analysis of P0 limbs. Gross morphology of the forelimbs (*E* and *F*) and hindlimbs (*G* and *H*) of littermates was similar in wild-type and *Msx2-Cre;Smo*$^{flox/flox}$ limbs animals. s, scapula; ss, spine of the scapula; h, humerus; dt, deltoid tuberosity; r, radius; u, ulna; a, autopod; il, ilium; is, ischium; f, femur; p, patella; t, tibia; fi, fibula.

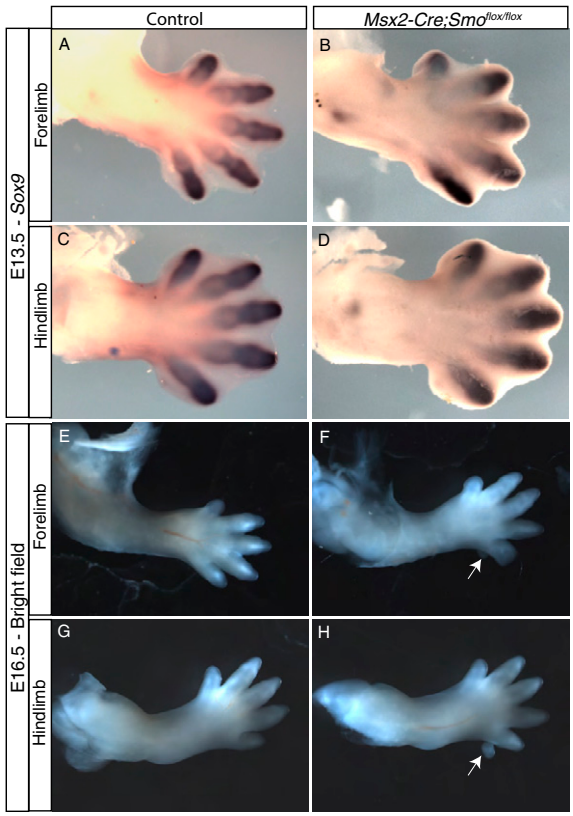

Fig. S6. Extra condensations form in *Msx2-Cre;Smo*$^{flox/flox}$ limbs between E13.5 and E16.5. To further investigate the extra cartilaginous condensation formed in *Msx2-Cre;Smo*$^{flox/flox}$ limbs, limbs were analyzed at E13.5 for expression of *Sox9* and at E16.5 by bright field microcopy. In both forelimbs (*A* and *B*) and hindlimbs (*C* and *D*), *Sox9* expression in *Msx2-Cre;Smo*$^{flox/flox}$ limbs and control limbs by whole-mount RNA in situ hybridization were found to be similar. However, analysis of forelimbs (*E* and *F*) and hindlimbs (*G* and *H*) by bright field microscopy revealed an extra cartilaginous condensation at E16.5 in the posterior of *Msx2-Cre;Smo*$^{flox/flox}$ limbs (see arrows in *F* and *H*).

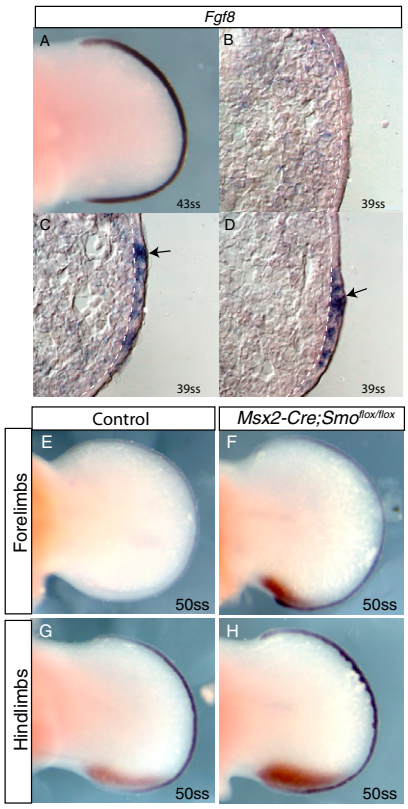

Fig. S7. *Fgf8* is expressed within the morphologically distinct AER in the developing limb. To confirm previous reports that *Fgf8* was expressed throughout the entire AER, limbs were analyzed by RNA in situ hybridization for expression of *Fgf8*. (*A*) Analysis of *Fgf8* expression revealed robust expression throughout the AER in 43ss hindlimbs. (*B*) Analysis of *Fgf8* expression on serial sections from embryos at 39ss revealed that when the ectoderm was a simple epithelial layer, no *Fgf8* was expressed. (*C* and *D*) However, *Fgf8* was expressed when the epithelium was stratified, which is indicative of an AER. White dashed line denotes the boundary between mesenchyme and epithelium. *B–D* were taken at the same magnification. (*E–H*) Double-labeled RNA in situ hybridizations on control and *Msx2-Cre;Smo*$^{flox/flox}$ limbs using a riboprobe against *Fgf8* (purple) and *Shh* (red) at 50ss. (*E* and *F*) In forelimbs, the AERs was longer, *Fgf8* expression was more robust and *Shh* expression was maintained in *Msx2-Cre;Smo*$^{flox/flox}$ limbs when compared with somite-matched controls. (*G* and *H*) In hindlimbs, AERs were longer and *Shh* expression was more robust in *Msx2-Cre;Smo*$^{flox/flox}$ limbs when compared with somite-matched controls.

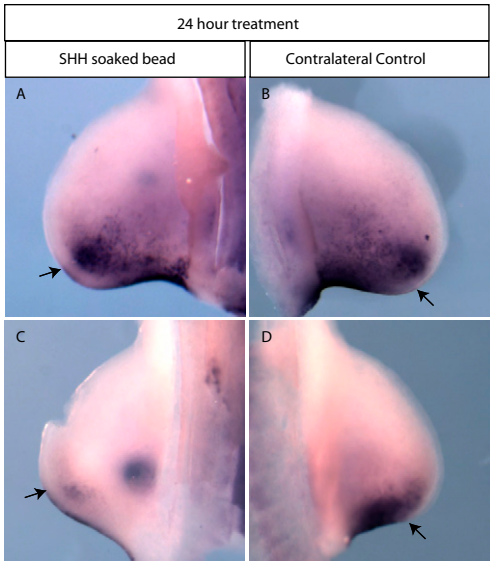

Fig. S8. *Ptch1* expression is expanded anteriorly within the AER after treatment with SHH-soaked beads. To determine whether an increase in SHH protein in the posterior of the limb resulted in expanded activation of the Hh signaling pathway in the ectoderm, limbs were treated with beads soaked in SHH protein and analyzed for expression of *Ptch1* by whole-mount RNA in situ hybridization (see *Methods* for more detail). After 24 h of treatment with a SHH-soaked bead, *Ptch1* expression was expanded anteriorly in the posterior AER (*A* and *C*) when compared with the contralateral control (*B* and *D*) (see arrows).

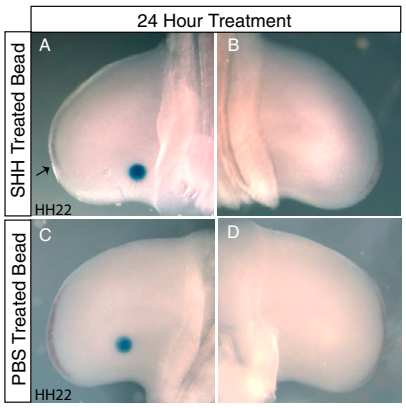

Fig. S9. *Fgf4* is excluded from the posterior AER after treatment with SHH-soaked beads. To determine whether increased SHH protein in the posterior of the limb altered the domain of *Fgf4* expression, we treated limbs with beads soaked in SHH (see *Methods* for more detail). After 24 h of treatment with a SHH-soaked bead, *Fgf4* expression was reduced in the posterior AER (*A*; arrow) when compared with the contralateral control (*B*). PBS soaked beads had no effect on the expression of *Fgf4* (*C* and *D*).

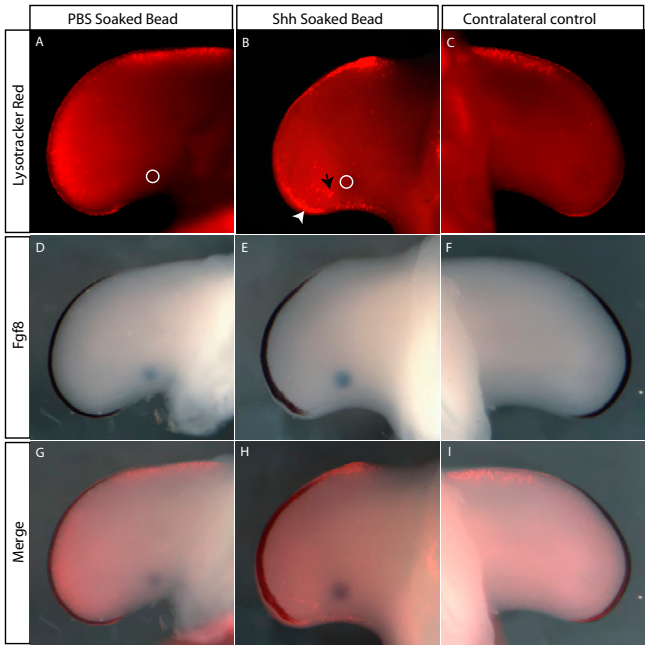

Fig. S10. Analysis of cell death in limbs that have been treated with SHH-soaked beads. To determine whether increased SHH protein in the posterior of the limb induced changes in cell death, we analyzed cell death by using LysoTracker red in limbs treated with a SHH-soaked bead (see *Methods* for more detail). (*A* and *C*) Analysis of cell death in limbs after treatment with PBS or in an untreated contralateral control revealed cell death in the anterior necrotic zone and the AER. After 24 h of treatment with a SHH-soaked bead, cell death was noticeably increased in the posterior of the limb including the mesoderm and AER (9/13 limbs; *B*). In *A* and *B*, white circles depict bead placement. The black arrow in *B* highlights cell death in the posterior of the limb bud, and the white arrowhead highlights cell death in the posterior AER. To determine the effect of a SHH bead on *Fgf8* expression, we analyzed *Fgf8* expression in the same limb buds used in *A*–*C*. (*D* and *F*) *Fgf8* expression was unaffected by treatment with a PBS-soaked bead or in a contralateral control limb. (*E*) Treatment with a SHH-soaked bead reduced the domain of *Fgf8* expression in the developing limb bud. (*G* and *I*) Merged images reveal that in a PBS-treated limb and a contralateral control limb, cell death can be detected at the anterior and posterior extremes of the domain of *Fgf8* expression. Treatment with a SHH-soaked bead resulted in a noticeable increase in cell death with most of the observed increase in cell death occurring at the anterior and posterior extremes of the domain of Fgf8 expression (*H*).

Table S1. Frequency of skeletal element number in forelimbs and hindlimbs of control and mutant animals

Limb	Genotype	No. of limbs observed	Digits in the autopod *n* (%)		
			Six	Five	Less than five
Forelimb	Control	18	0	18 (100)	0
	Msx2-Cre;Smo$^{flox/flox}$*	10	8 (80)	2 (20)	0
Hindlimb	Control	18	0	18 (100)	0
	Msx2-Cre;Smo$^{flox/flox}$*	10	9 (90)	1 (10)	0

*Msx2-Cre samples were analyzed immediately after fixation and before skeletal preparation because of potential loss of extra tissue during the clearing process.